Defence Research and Development Canada
Recherche et développement pour la défense Canada

DEFENCE R&D DÉFENSE

Focusing Moving Targets

Terrain imaged with moving-target matched filters: A tutorial

Chuck Livingstone and Ishuwa Sikaneta

Defence R&D Canada – Ottawa
TECHNICAL MEMORANDUM
DRDC Ottawa TM 2004-160
September 2004

Canada

Focusing moving targets

Terrain imaged with moving-target matched filters: A Tutorial

Chuck Livingstone and Ishuwa Sikaneta

Defence R&D Canada - Ottawa

Technical Memorandum

DRDC Ottawa TM 2004-160

September 2004

Abstract

This technical memorandum provides a tutorial on the processing of synthetic aperture radar (SAR) ground moving target indication (GMTI) data with a filter that is not matched to the collected data. This could occur, for example, when objects in the terrain undergo motion that is not accounted for in the SAR filter. Or, conversely, when the SAR filter has been modified to compress moving objects thereby introducing a mismatch with stationary objects.

Additionally, due to the sampling of the SAR signal, ambiguities become an issue. The matched filter to properly focus an image is not unique. It is possible that a filter constructed with a given across-track velocity parameter yields a SAR image that cannot be distinguished from the SAR image constructed with a filter identical in all respects except for a different but appropriately chosen across-track velocity parameter. This technical memorandum explores the ambiguity issue and discusses the impact on SAR-GMTI.

Résumé

Le présent document technique constitue un document d'apprentissage sur le traitement, à l'aide d'un filtre non adapté aux données recueillies, des données d'indication de cibles terrestres mobiles (GMTI) fournies par un radar à synthèse d'ouverture (SAR), par exemple lorsque des objets sur le terrain subissent des mouvements qui ne sont pas pris en compte dans le filtre SAR ou, à l'inverse, lorsque le filtre SAR a été modifié pour appliquer une compression aux objets mobiles, ce qui crée une désadaptation dans le cas des objets fixes.

En outre, en raison de l'échantillonnage du signal SAR, les ambiguïtés deviennent un problème. Le filtre adapté servant à la focalisation adéquate d'une image n'est pas unique. Il est possible qu'un filtre construit avec un paramètre de vitesse transversale donnée fournisse une image SAR qui ne peut pas être distinguée de l'image SAR construite avec un filtre identique à tous les points de vue, sauf pour ce qui est d'un paramètre de vitesse transversale différente mais correctement choisie. Le présent document technique examine le problème d'ambiguïté et traite de ses répercussions sur la GMTI par SAR.

This page intentionally left blank.

Executive summary

This technical memorandum provides a tutorial on the signal processing of SAR data for GMTI. Adaptation to the SAR filter to allow for correct focusing of moving targets introduces an incorrect filter for stationary objects. Or, in the opposite case, the filter used to correctly focus stationary objects is not suitable for moving objects. Issues of an incorrectly selected SAR filter are explored, especially as they pertain to GMTI.

Another issue associated with SAR GMTI data stems from the sampled nature of the SAR data at the pulse repetition frequency. Moving objects are ambiguous in their across-track velocity component due to the finite sampling rate. For example, it is possible that the SAR image of an object with a given across-track velocity is indistinguishable from the SAR image of the same object at a different across-track velocity; the difference between the two velocities is some multiple of what is known as the wrap velocity. This technical memorandum presents the physics of the wrap velocity.

Overall, this technical memorandum aids in understanding the physical processes measured by the SAR data, particularly those due to moving objects.

Chuck Livingstone and Ishuwa Sikaneta; 2004; Focusing moving targets;
DRDC Ottawa TM 2004-160; Defence R&D Canada - Ottawa.

Sommaire

Le présent document technique constitue un document d'apprentissage sur le traitement des signaux de données SAR pour la GMTI. La modification du filtre SAR pour permettre la focalisation correcte des cibles mobiles signifie que le filtre devient inapproprié pour les objets fixes. à l'inverse, le filtre utilisé pour focaliser correctement les objets fixes n'est pas adéquat pour les objets mobiles. Les problèmes de sélection inappropriée d'un filtre SAR sont examinés, en particulier en rapport avec la GMTI.

Un autre problème concernant les données de GMTI par SAR découle de l'échantillonnage des données SAR à la fréquence de répétition des impulsions. Les objets mobiles présentent une ambiguïté quant à la composante de vitesse transversale en raison du taux d'échantillonnage fini. Par exemple, il est possible que l'image SAR d'un objet ayant une vitesse transversale donnée ne puisse être distinguée de l'image SAR du même objet ayant une vitesse transversale différente, la différence entre les deux vitesses étant un multiple de ce qu'on appelle la vitesse d'enveloppe. Le présent document technique expose les caractéristiques physiques de la vitesse d'enveloppe.

Dans l'ensemble, le présent document technique aide à comprendre les processus physiques mesurés à l'aide des données SAR, en particulier ceux qui sont dus aux objets mobiles.

Chuck Livingstone and Ishuwa Sikaneta; 2004; Focusing moving targets;
DRDC Ottawa TM 2004-160; R & D pour la défense Canada - Ottawa.

Table of contents

List of figures

This page intentionally left blank.

1 Introduction

This tutorial addresses two issues that arise in the processing of dual channel SAR data for GMTI. The first issue concerns impulse response width broadening. We seek to identify the theoretical pulse broadening when stationary terrain is processed by a moving-target matched filter or when a moving target is processed by a stationary-world matched filter. The second issue, concerning terrain and GMTI ambiguities, arises from the sampled nature of the SAR data and motivates the following question: what are the along-track interferometric (ATI) properties of terrain ambiguities when the processing filter is matched to a moving target?

2 Development for airborne observations of a range-compressed moving target with a stationary-world matched filter – SAR processing with a mismatched filter

2.1 Signal phase

The moving-target phase for an airborne SAR imaging a plane earth [1] can be written as:

$$\varphi_T = \frac{4\pi}{\lambda}\left[\sqrt{(a_T^2+b_T^2)\left(t+\frac{b_T y_0}{a_T^2+b_T^2}\right)^2 + R_0^2 - \frac{b_T^2 y_0^2}{a_T^2+b_T^2}} - R_0\right] \tag{1}$$

for $a_T = V_a - V_x$, $b_T = V_y$; V_x is parallel to the flight direction, V_y is along the surface normal to the flight direction. V_a is the aircraft velocity

Expand the products and divide through by R_0^2

$$\varphi_T = \frac{4\pi R_0}{\lambda}\left[\sqrt{1+\frac{a_T^2+b_T^2}{R_0^2}t^2+\frac{2b_T y_0}{R_0^2}t} - 1\right]. \tag{2}$$

Expand $\sqrt{1+x} = 1+\frac{x}{2}-\frac{x^2}{8}+etc$ for $x << 1$, substitute a_T and b_T, and normalize to V_a

$$\varphi_T = \frac{2\pi V_a^2}{\lambda R_0}\left[1\left(-2\frac{V_x}{V_a}+\frac{V_x^2}{V_a^2}+\frac{V_y^2}{V_a^2}\right)t^2 + 2\frac{V_y y_0}{V_a}t\right] \tag{3}$$

For plane-earth geometry $y_0/R_o = \sin(\psi)$ for incidence angle ψ when y_0 is the ground-range offset of the target.

Noting that the radial velocity, V_R, of the target is given by:

$$V_R = V_y \sin\psi, \tag{4}$$

the linear phase term becomes $2\pi f_D t = \omega_D t$ for Doppler frequency, f_D, that results from the radial velocity, V_R, of the target.

By setting $k_0 = \frac{2\pi V_a^2}{\lambda R_0}$, target phase term becomes:

$$\Phi_T = k_0 \left(1 + \frac{V_y^2}{V_a^2} + \frac{V_x^2}{V_a^2} - 2\frac{V_x}{V_a}\right) t^2 + \omega_D t. \tag{5}$$

2.2 Signal model

If the signal amplitude is given by the real function, a(t), the time-domain signal from the target has the form:

$$s_T = a(t) \exp\left[k_0 \left(1 + \frac{V_y^2}{V_a^2} + \frac{V_x^2}{V_a^2} - 2\frac{V_x}{V_a}\right) t^2 + \omega_D t\right], \tag{6}$$

where $a(t)$ represents the target return magnitudes over the total observation period for a moving target. It is determined by the radar equation for range compressed data and the signal path gain as

$$a(t) = \sqrt{\frac{P_t \lambda^2 G_t(\phi,\theta) G_r(\phi,\theta) \sigma_{targ}(\theta) g_{sys}}{4\pi^3 R^4}},$$

where $P_t$is the transmitted power, λ is the radar wavelength, G_t andG_r are the transmit and receive antenna gains, ϕ is the elevation angle at the antenna, $\theta(t)$ is the azimuth angle at the antenna for $t = x/V_a$, σ_{targ} is the target cross section, g_{sys} is the radar system gain (including propagation path losses) and R is the range to the observation point at angles ϕ,θ.

From the point of view of the shape of the function over a limited range interval it can be considered to be composed of the peak of the antenna pattern modulated by the target return amplitude. For the sake of simplicity we will assume that the target returns have constant amplitude over the azimuth observation window and that the shape of $a(t)$ is defined by the azimuth antenna pattern. For satellite radars we are looking at the main lobe of the antenna pattern from an almost uniformly illuminated array and we can approximate $a(t)$ by

$$a(t) = \left(a \frac{\sin \frac{t\pi}{T}}{\frac{t\pi}{T}} \right)^2 = A\text{sinc}^2 \frac{t}{T} \tag{7}$$

This approximation is less accurate for airborne radars where spatial weighting is applied to suppress azimuth side-lobes, however, near the peak of the antenna pattern, the approximation is usable if T is scaled.

For a sinc function, T is half of the separation of the first two nulls. For an antenna pattern, the beamwidth is usually defined as the –3dB amplitude of the one-way antenna pattern and is related to time (in the azimuth direction) by the motion of the radar as shown in equations (8) and (9).

2.3 Beamwidth

If the antenna beamwidth is θ_0 , the broadside-range to the observation point is R_0, and the radar velocity is V_a, the time required for the beam to pass an observation point is given by

$$2\tau = \frac{R_0 \theta_0}{V_a} \tag{8}$$

For a sinc function, the -3db half-width is related to the distance to the first nulls by 0.44295 or for our model case,

$$T = 2.25759\tau \tag{9}$$

2.4 Bandwidth

The nominal bandwidth (radians/second) of the signal, 2Ω, is defined at the -3dB width to be

$$\Omega = 2k_0\tau \left(1 + \frac{V_y^2}{V_a^2} + \frac{V_x^2}{V_a^2} - 2\frac{V_x}{V_a} \right) \tag{10}$$

Looking at the target velocity terms we see that the bandwidth is most sensitive to the azimuth velocity. We will look at the impact of that later. For slowly moving targets, the signal bandwidth lies very close to that for the stationary world. In this case,

$$\Omega \approx 2k_0\tau = \frac{2\pi V_a \theta_0}{\lambda} \tag{11}$$

Radar systems are often discussed in terms of their time-bandwidth product. For slowly moving targets this is

$$B = \frac{4\tau\Omega}{2\pi} \approx \frac{4k_0\tau^2}{\pi} = \frac{2R_0\theta_0^2}{\lambda} \tag{12}$$

2.5 Sampling

Because the antenna pattern is a continuously varying function, the bandwidth and duration computed from it define "soft" limits that are somewhat arbitrary. The reality is that the azimuth signal received by the radar is not the continuous function expressed above but is a sampled function where the sampling rate is arbitrarily set to adequately sample the selected band limit. In normal practice, radar pulse repetition frequencies, f_s, are selected to over-sample the selected beam-width by factors in the range 1.1 to 1.3. Assuming 0-mean (base-band) signal spectra, the continuous nature of the signal being sampled results in spectral components outside of the selected bandwidth being aliased into the central spectral region. These aliased signals are the azimuth sampling ambiguities or "azimuth ambiguities" of the signal data. For signal $s_T(t)$ with spectrum $S_T(f)$, spectral components in the frequency range $-3f_s < f < -f_s$ are mapped into the frequency range $-f_s < f + 2f_s < f_s$and spectral components in the frequency range $f_s < f < 3f_s$ are also mapped into the frequency range $-f_s < f - 2f_s < f_s$. These are the first-order ambiguities and these aliased spectra carry with them the properties corresponding to their central squint angles.

Noting that the Doppler frequency that corresponds to the -3dB point of the antenna pattern is $f_D = \frac{k_0\tau}{\pi}$ and that $f_s > f_D$ we define the over-sampling-ratio as $O = f_s/f_D$. The time interval that corresponds to the Nyquist sampling frequency f_s is $\tau_s = O\tau$. Following the same arguments, the maximum sampled bandwidth is $\Omega_s = O\Omega$.

From the point of view of the signal spectrum, the sampling process applies a hard limit to the sampled bandwidth and thus to the time window for any spectral manipulation. The appropriate spectral representation is a discrete Fourier series. In the remaining discussions the signal will not be expanded in its sampled form to keep the discussion simple.

2.6 Signal spectrum

The signal spectrum is defined as

$$S(f) = F(s(t)) = F\left\{a(t)\exp\left[k_0\left(1 + \frac{V_y^2}{V_a^2} + \frac{V_x^2}{V_a^2} - 2\frac{V_x}{V_a}\right)t^2 + \omega_D t\right]\right\} \quad (13)$$

where $F()$ is the integral Fourier transform operator. Defining:

$$\Omega_s = 2\pi f_s,\ \omega = 2\pi f, \alpha = 1 + \frac{V_y^2}{V_a^2} + \frac{V_x^2}{V_a^2} - 2\frac{V_x}{V_a}, \quad (14)$$

and applying the frequency shifting theorem of the Fourier transform and the method of stationary phase [2], we have a sampled spectrum whose continuous representation is

$$S(f) = \begin{cases} 2\pi\Omega_s\sqrt{\frac{\pi}{k_0\alpha_D}}A(\omega+\omega_D)e^{j\frac{\omega-\omega_D}{4k_0\alpha}-\frac{\pi}{4}} & -\Omega_s+\omega_D < \omega+\omega_D < \Omega_s+\omega_D \\ 0 & \text{otherwise.} \end{cases} \tag{15}$$

where $P_{\Omega_s}(\omega-\omega_D)$ is the unit impulse function of width $2\Omega_s$ centred at ω_D and $A(\omega-\omega_D)$ is the shape of the spectrum defined by $a(t)$. The function "A" is defined by the time history of the target illumination and does not depend on the radial velocity of the target. As the analog signal is sampled over a fixed bandwidth, and as there is signal energy outside of this bandwidth, the sampled signal lying outside of the interval defined by $P_{\Omega_s}(\omega-\omega_D)$ is folded into the spectrum $S(f)$ by the rule:

$$|\omega+\omega_D| > \Omega_s,\ (\omega+\omega_D) \rightarrow 2\Omega_s \text{sgn}(\omega+\omega_D)\text{floor}\left(\left|\frac{\omega+\omega_D}{\Omega_s}\right|\right)+\omega+\omega_D \tag{16}$$

In SAR processing, these become the azimuth ambiguities discussed in section 2.4. Following the discussion in section 2.5, the sampling process maps the spectral interval $-\Omega_s-\omega_D$ to $\Omega_s-\omega_D$ to the 0-centred interval $-\Omega_s < \omega' < \Omega_s$. When the signal bandwidth is less than or equal to $2\Omega_s$, ω_D defines the position of the centre of the spectrum and $\omega_D \neq 0$ causes the spectrum to wrap in the direction defined by the sign of ω_D. When $\omega_D = \Omega_s$ the central region of the spectrum is mapped to Ω_s and $-\Omega_s$ and the edges of the spectrum are mapped to -0 and +0. The spectral mapping for ω_D = $2\Omega_s$ is the same as that for $\omega_D = 0$ or the spectrum is ambiguous (with the exception of the FM constant) in ω_D. When $|\omega_D| > \Omega_s$ the spectrum is ambiguous in the sign of ω_D

The ambiguities are similarly wrapped.

2.7 Stationary world matched filter

A point on the stationary world has a phase history of the form $e^{-jk_0t^2}$ centred at $t = 0$ for sampled time $-\tau < t < \tau$. $\tau = \tau_s$ defines the Nyquist sampling limit. When no spectral amplitude weighting is used for side-lobe control, the matched filter spectrum has the form:

$$H(f) = P_\Omega(\omega)e^{-j\frac{\omega^2}{4k_0^2}-j\frac{\pi}{4}} \tag{17}$$

In normal practise $\Omega < \Omega_s$ to block the strongest ambiguous signals and an amplitude weighting function $B(f)$ or non-linear FM, $k(t)$ is used for side-lobe suppression. In this analysis, the weighting is assumed to be unity.

2.8 SAR Image Spectrum

The SAR image spectrum is defined by the product $I(f) = S(f)H(f)$. In expanded form (before considering the sampling process,) this is

$$I(f) = 2\pi\Omega_s\sqrt{\frac{\pi}{k_0\alpha}}A(\omega+\omega_D)P_{\Omega_s}(\omega+\omega_D)P_{\Omega}(\omega)\exp j\left(\frac{(\omega+\omega_D)^2}{4k_0\alpha}-\frac{\omega^2}{4k_0^2}\right) \tag{18}$$

2.8.1 Target Amplitude terms

Examining the amplitude terms, the functions P_{Ω_s} and P define hard spectral limits for the target and the matched filter respectively, while the function A is determined by the illumination history of the target and is only weakly coupled to the target motion through the targets' "x" velocity component.

If the wrapping effects of the sampling operation are ignored for a moment, the radial velocity of the target acts to shift the target spectrum and, thus select the interval of A that contributes to the target signal strength. As the magnitude of the radial velocity of the target (and, thus, $|\omega_D|$) increases, $A(\omega+\omega_D)P_{\Omega_s}(\omega+\omega_D)\cap P(\omega)$ eventually decreases thus decreasing the target energy until, eventually there is no overlap and the target response is 0.

Graphically, the target energy (and thus amplitude) would have the form shown in figure 1 as ω_D varies over the range $-\Omega_s-\Omega$ to $\Omega_s+\Omega$.

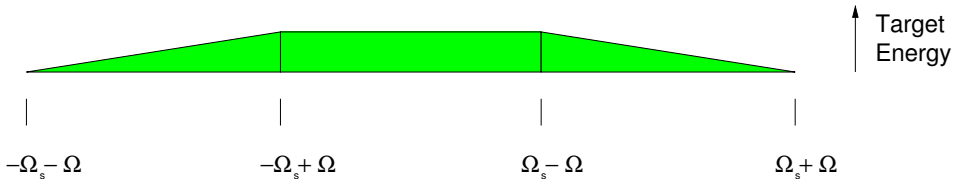

Figure 1: *Schematic representation of the energy in a SAR processed target with mismatched signal and processing spectra and hard spectral limits but without spectral wrapping from sampling*

In the real (sampled) world, $P_{\Omega_s}(\omega+\omega_D)$ maps into $P_{\Omega_s}(\omega)$ as the sum of two terms, each with its own phase structure. Continuing the complex signal convention of positive and negative frequencies we can write:

$$P_{\Omega_s}(\omega+\omega_D) \rightarrow P_{\Omega_s}(\omega) = P_{\Omega_s-\omega_D/2}(\omega+\omega_D)+P_{\omega_D/2}(-2\Omega_s\text{sgn}(\omega+\omega_D)+\omega+\omega_D) \tag{19}$$

Equation 19 is valid for signals spanning the first azimuth ambiguity. For $\omega_D > 0$: the minimum value of $\omega + \omega_D$ is $-\Omega_s + \omega_D$ and the maximum value is Ω_s, and $-2\Omega_s \text{sgn}(\omega + \omega_D) + \omega + \omega_D$ lies in the range $-\Omega_s$ to $-\Omega_s + \omega_D$. For $\omega_D < 0$: the minimum value of $\omega + \omega_D$ is $-\Omega_s$ and the maximum value is $\Omega_s + \omega_D$ and $-2\Omega_s \text{sgn}(\omega + \omega_D) + \omega + \omega_D$ lies in the range $\Omega_s + \omega_D$ to Ω_s. A graphical representation of the mapping process is shown in figure 2.

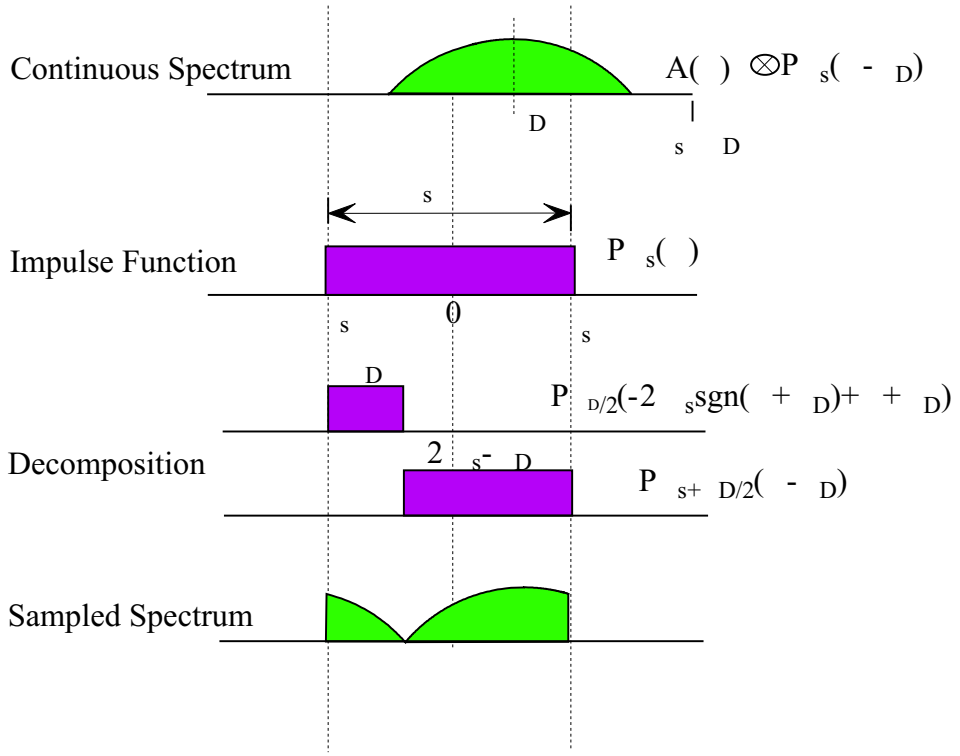

Figure 2: *Schematic representation of the wrapping of a shifted signal spectrum caused by sampling.*

The impulse function of the processing filter, $P_\Omega(\omega)$ is normally chosen to be narrower than the Nyquist sampling range. When the processing filter is chosen to process the stationary world, it selects the sampled SAR spectrum interval centred at 0 Hz. If the processing filter is matched to the target, it wraps around the sampling interval in the same manner as the signal spectrum. In this section we are considering the stationary world case.

The product $A(\omega + \omega_D)P_\Omega(\omega + \omega_D)P_\Omega(\omega)$ determines the spectral interval that is processed to generate the target signal. Applying the signal impulse function decomposition associated with the signal sampling, $P_{\Omega_s}(\omega + \omega_D)$ becomes the sum of two impulse functions, each of which has its own phase function. Ignoring the

phase functions, we have:

$$A(\omega+\omega_D)\left(P_{\Omega_s-\omega_D/2}(\omega+\omega_D)+P_{\omega_D/2}(-2\Omega_s\text{sgn}(\omega+\omega_D)+\omega+\omega_D)\right)P_\Omega(\omega). \tag{20}$$

The intersections of the signal impulse functions with the matched filter impulse function define two domains. While $|\omega_D| < \Omega_s - \Omega$ or $2\Omega_s < |\omega_D| < \Omega_s + \Omega$, the smaller (wrapped) domain is not in the intersection of the impulse functions and the product only contains one spectral interval. Otherwise, there are two valid intersection regions whose phase functions define different spectral intervals. After inverse transformation, these spectra define two, spatially separated targets whose strengths are related to the spectral power captured by each impulse function in the intersection interval. For $\omega_D < \Omega_s$, the stronger target is the "true" target and the weaker target is ambiguous. For $\omega_D = \Omega_s$, the two targets have equal magnitude and are truly ambiguous. When $\omega_D \geqslant \Omega_s$, the sign of ω_D becomes ambiguous and the stronger target is the ambiguous one. These relationships are illustrated in figure 3.

In addition to selecting the segments of the wrapped signal spectrum that are processed to form a SAR image, the impulse function intersections also define the bandwidth and spectral amplitude distribution associated with each target. The spectral bandwidth and spectral weighting within each of the two intersections are factors in the determination height and width of the focused pulse.

2.8.2 Target phase terms

The impulse function intersections select the spectral intervals in the associated phase functions. To simplify the resulting expressions set:

$$\Omega_1 = \Omega_s - \frac{\omega_d}{2},\ \Omega_2 = \frac{\omega_D}{2},\ \omega'_D = -\frac{\Omega_s+\Omega-\text{sgn}(\omega_D)}{2} \tag{21}$$

Capturing the constant amplitude terms in equation (18) in $A(\omega-\omega_D)$, the resulting image spectrum then takes the form:

$$\begin{aligned} I(f) = A(\omega+\omega_D)\Bigg(& P_{\Omega_1}(\omega+\omega_D)P_\Omega(\omega)\exp j\left(\frac{(\omega+\omega_D)^2}{4k_0\alpha}-\frac{\omega^2}{4k_0^2}\right) \\ & +P_{\Omega_2}(\omega+\omega'_D)P_\Omega(\omega)\exp j\left(\frac{(\omega+\omega'_D)^2}{4k_0\alpha}-\frac{\omega^2}{4k_0^2}\right)\Bigg) \end{aligned} \tag{22}$$

Noting that $\alpha \approx 1$ we can represent $1/\alpha$ as the first term of the series for $1/(1+x)$ and the expansion of the phase of the first term becomes:

$$\phi_1(\omega) = \left\{ \frac{1}{4k_0}\left[(\omega+\omega_D)^2\left(1+\frac{V_y^2}{V_a^2}+\frac{V_x^2}{V_a^2}-2\frac{V_x}{V_a}\right)-\omega^2\right] \quad \text{for } -\Omega \leq \omega+\omega_D \leq \Omega \right. \tag{23}$$

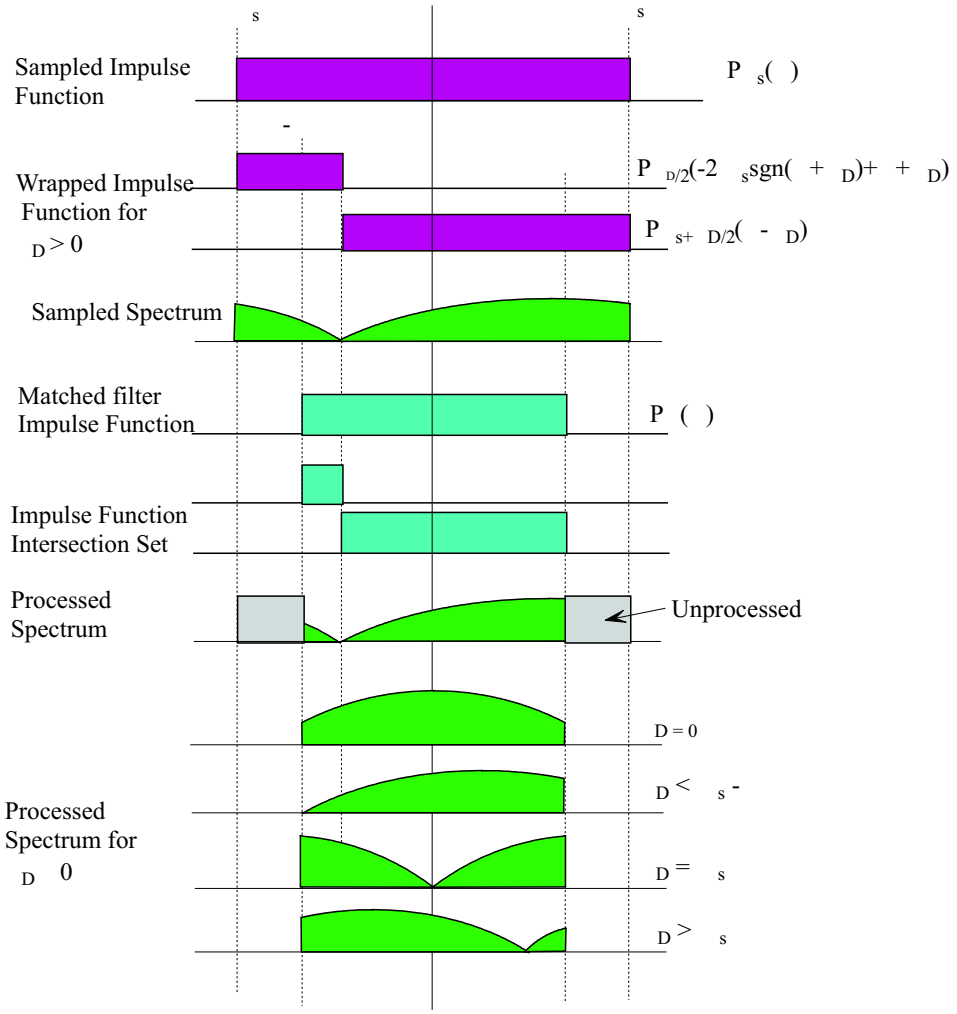

Figure 3: *Schematic representation of the sampled signal spectrum of a target and the SAR processed spectrum as ω_D is varied for over-sampling ratio $\Omega_s/\Omega = 1.42$*

Applying the same treatment to the second term we have:

$$\phi_2(\omega) = \left\{ \frac{1}{4k_0} \left[(\omega + \omega'_D)^2 \left(1 + \frac{V_y^2}{V_a^2} + \frac{V_x^2}{V_a^2} - 2\frac{V_x}{V_a} \right) - \omega^2 \right] \right. \quad \text{for } -\Omega \leq \omega + \omega'_D \leq \Omega \tag{24}$$

There are two cases of interest with somewhat different properties: $V_x = 0$ and $V_y = 0$

2.8.2.1 The radial velocity case

Starting with the case $V_x = 0$,

$$\phi_1(\omega) = \frac{1}{4k_0} \left[\omega^2 \frac{V_y^2}{V_a^2} + 2\omega\omega_D \left(1 + \frac{V_y^2}{V_a^2} \right) + \omega_D^2 \left(1 + \frac{V_y^2}{V_a^2} \right) \right] \tag{25}$$

The phase equation for the second term in equation (22) has an identical form with ω_D replaced by ω'_D.

Looking at the terms in equation (25) from the viewpoint of the "focused" target, the first term, $\omega^2 \frac{V_y^2}{4k_0 V_a^2}$, is a focus error term and contributes to the focused target peak while $\omega^2 \frac{V_y^2}{4k_0 V_a^2} < \frac{\pi}{2}$. Substituting for k_0 we see that the focus constraint

$$|\omega| \leq \frac{\pi V_a}{\sqrt{\lambda R_0}} \left(\frac{V_a}{V_y} \right) = \omega_f \tag{26}$$

is most significant at long range when V_y/V_a is large. For airborne radars viewing fast-moving targets the pair of constraints

- $-\Omega \leq \omega + \omega_D \leqslant \Omega$ defined by $P_{\Omega_1}(\omega + \omega_D) P_\Omega(\omega)$ and
- $|\omega| \leq \omega_f$

define the focused bandwidth and, thus, the temporal (spatial) width of the focused target.

The second term of (25) defines a time-frequency product of the form $t_0\omega = \omega \frac{\omega_D}{2k_0} \left(1 + \frac{V_y^2}{V_a^2} \right)$, where t_0 is a time offset. The final stage of SAR processing is an inverse Fourier transform and from the time shifting theorem of the Fourier transform $G(\omega)e^{j\omega t_0} \leftrightarrow g(t + t_0)$ where the time (space) shift is

$$t_0 = \frac{\omega_D}{2k_0} \left(1 + \frac{V_y^2}{V_a^2} \right), \quad \forall |\omega_D| \leq \Omega_s - \Omega \tag{27}$$

$$t_1 = \frac{(\Omega - \Omega_s)\text{sgn}(\omega_D) + \omega_D}{4k_0} \left(1 + \frac{V_y^2}{V_a^2} \right), \quad \forall \{\Omega_s - \Omega < |\omega_D| < \Omega_s + \Omega\} \tag{28}$$

The third term of (25) is a constant phase shift that depends on ω_D, and is not changed through the inverse transform process.

When the second term of (22) is expanded under the condition $V_x = 0$, the resulting phase, ϕ_2, has the same form as (25) with ω_D replaced by ω'_D. The discussion of focus effects remains unchanged except that a different spectral region and width, defined by $P_{\Omega_2}(\omega + \omega'_D)P_\Omega(\omega)$ is in force. For ϕ_2, the target shift term becomes

$$t'_0 = \frac{\omega'_D}{2k_0}\left(1 + \frac{V_y^2}{V_a^2}\right) = \frac{-\Omega_s - \Omega + \omega_D \text{sgn}(\omega_D)}{4k_0}\left(1 + \frac{V_y^2}{V_a^2}\right) \tag{29}$$

which defines a separate target shifted in the opposite direction. The constant phase term is also changed by the substitution of ω_D by ω'_D.

2.8.2.2 The tangential velocity case

When we apply the condition $V_y = 0$ to equations (23) and (24) we alter the significance of the target velocity in the target phase calculation as the dominant radial velocity term given by (4) and, thus, ω_D are now 0. The resulting signal spectrum becomes:

$$S(f) = 2\pi\Omega_s\sqrt{\frac{\pi}{k_0\alpha}}A(\omega)P_{\Omega_s}(\omega)e^{j\left(\frac{\omega^2}{4k_0\alpha} - \frac{\pi}{4}\right)} \tag{30}$$

The image spectrum now becomes:

$$I(f) = 2\pi\Omega_s\sqrt{\frac{\pi}{k_0\alpha}}A(\omega)P_{\Omega_s}(\omega)e^{j\frac{\omega^2}{4k_0}\left(\frac{1}{\alpha} - 1\right)} \tag{31}$$

As the amplitude terms are both centred at 0, the wrapping effects of the previous ω_D offset are no longer observed.

Expanding $1/\alpha$ in the phase term, we find

$$\phi = \frac{\omega^2}{4k_0}\left(-2\frac{V_x}{V_a} + \frac{V_x^2}{V_a^2}\right) \tag{32}$$

As $|V_x/V_a| < 1$, V_x/V_a is more significant than V_y^2/V_a^2 in determining the target focus. When V_x andV_a are in the same direction, the effective aperture time for the moving target is increased and the sign of the residual FM rate is reversed. When V_x and V_a are oppositely directed, the effective aperture time for the target is reduced but the sign of the residual FM rate is unchanged.

Applying the focus phase constraint, $|\frac{\omega^2}{4k_0}\left(-2\frac{V_x}{V_a} + \frac{V_x^2}{V_a^2}\right)| \leq \frac{\pi}{2}$, focus error effects are seen to be stronger for motion parallel to the radar velocity than they are for

radial velocity and they are weakly dependent on the relative directions of platform and target motion. This will be particularly important for space-based radar systems.

The focus phase constraint will become significant when

$$|\frac{\Omega^2}{4k_0}\left(-2\frac{V_x}{V_a}+\frac{V_x^2}{V_a^2}\right)| > \frac{\pi}{2} \tag{33}$$

From equation (31), the angular frequency defined by the phase constraint is :

$$\Omega_\phi = \sqrt{\frac{2\pi k_0 \alpha}{1-\alpha}} = (V_a - V_x)\sqrt{\frac{2\pi k_0}{V_x(2V_a - V_x)}} \tag{34}$$

Any frequency $\Omega_\phi < \Omega$ constrains the effective width of $P_\Omega(\omega)$ and, thus, increases the impulse-response-width of the focused target.

As the image phase in equation (32) has no terms that are linear in ω and no constant phase terms, the moving target is not displaced from its beam centre position and has no residual phase shift caused by SAR processing when V_y = 0.

In practice the majority of moving targets have both radial and tangential velocity components and both effects discussed are apparent.

2.8.2.3 Fully ambiguous targets

From figure 3 we see that when target radial velocity yields Doppler shifts in the range

$\Omega_s \leq |\omega_D \leq 2\Omega_s$ the sign of ω_D is ambiguous. At ω_D = Ω_s the image spectrum becomes ambiguous with the spectrum for $\omega = 0$. The only difference between the two cases is the parameter α which continues to change with increasing V_y (and V_x) and the absolute phase of the target (which tracks the real target velocity). The intervals

$$\{-3\Omega_s < \omega \leq -\Omega_s\} \text{ and } \{\Omega_s \leq \omega < 2\Omega_s\} \tag{35}$$

define the first sampling (or azimuth) ambiguity domains. Within each of the ambiguous domains, the discussions for Figures 2 and 3 apply to targets in the same manner as they did for the unambiguous data. In the ambiguous domains the phase constraint discussed previously becomes progressively more significant in determining the impulse response width of the focused targets.

3 Development for airborne observations of a range-compressed stationary world with a moving target matched filter – SAR processing with a mismatched filter

The case of a stationary world processed with a moving target matched filter is similar to the case of a moving target matched filter but there are some important differences. For the present case, the image spectrum is stationary, the matched-filter is wrapped by the sampling process and the spectral skirts outside of the sampled interval fold into the spectrum at the same time as the main scene. For the moving target case this also occurs but at a significantly different time.

3.1 Terrain spectral amplitude terms

In comparison to (18), the image spectrum takes the form:

$$I(f) = 2\pi\Omega_s\sqrt{\frac{\pi}{k_0\alpha}}A(\omega)P_{\Omega_s}(\omega)P_{\Omega}(\omega+\omega_D)e^{j\left(\frac{\omega^2}{4k_0^2}-\frac{(\omega+\omega_D)^2}{4k_0\alpha}\right)} \tag{36}$$

ω_D is now part of the matched filter and is the moving target Doppler estimate. The antenna pattern influence on the stationary world spectrum that defines $A(\omega)$ contains elements beyond the sampling window impulse function that fold into the sampled spectrum as shown in figure 4.

In figure 4 we see that the sampled spectrum is a composite of unambiguous and ambiguous spectral components. Each of the ambiguous spectral components corresponds to terrain signals originating at a squint angle

$$\Psi = \pm\sin^{-1}\left(\frac{\lambda 2n\Omega_s}{V_a}\right) \tag{37}$$

where n is the order of the ambiguity, and, thus has its own amplitude and phase distribution. Extracting the terrain spectrum terms from equation (36), we have

$$\begin{aligned} A(\omega)e^{j\left(\frac{\omega^2}{4k_0}-\frac{\pi}{4}\right)} &= A_0(\omega_0)e^{j\left(\frac{\omega_0^2}{4k_0}-\frac{\pi}{4}\right)} \\ &+\sum_{n=1}^{N}\left(A_{n+}(\omega_{n+})e^{j\left(\frac{(\omega_{n+}-2n\Omega_s)^2}{4k_0}-\frac{\pi}{4}\right)}+A_{n-}(\omega_{n-})e^{j\left(\frac{(\omega_{n-}+2n\Omega_s)^2}{4k_0}-\frac{\pi}{4}\right)}\right) \end{aligned} \tag{38}$$

where N is the largest ambiguity order that contains significant signal power. For a well designed radar antenna, $N \approx 1$. Higher orders of N correspond to sidelobe

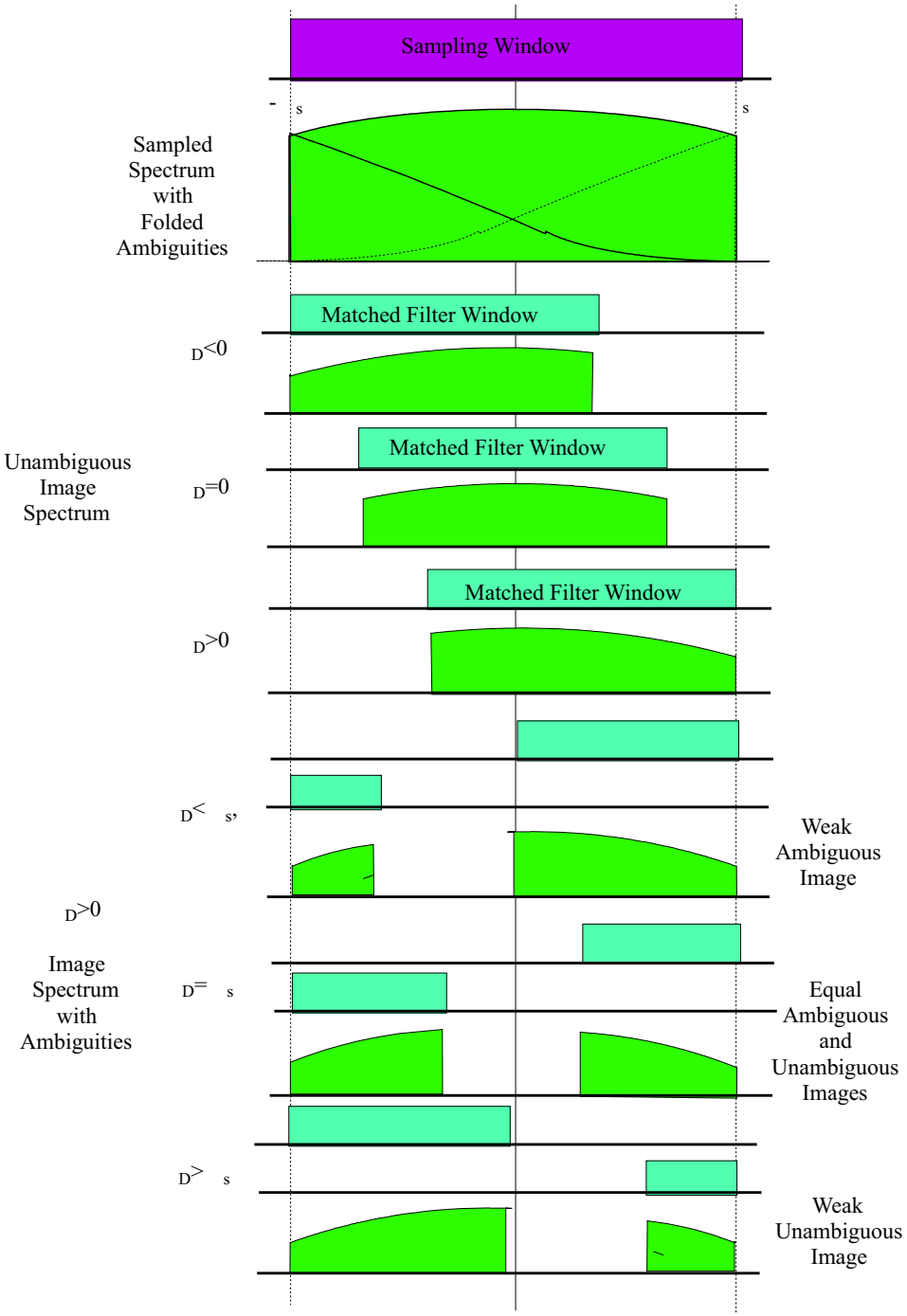

Figure 4: *Schematic representation of spectral folding and ambiguities in a sampled terrain spectrum*

structures and are too small to be of significance in most single-aperture SAR cases but can become important in DPCA images.

Examining the terms of (38), we have:

$$A_0(\omega) = A(\omega), \qquad \omega_0 = \omega \qquad \text{for} \quad -\Omega_s < \omega \leq \Omega_s \tag{39}$$

$$A_{1+}(\omega_{1+}) = A(\omega), \qquad \omega_{1+} = \omega \qquad \text{for} \quad \Omega_s \leq \omega < 3\Omega_s \tag{40}$$

$$A_{1-}(\omega_{1-}) = A(\omega), \qquad \omega_{1-} = \omega \qquad \text{for} \quad -3\Omega_s \leq \omega < -\Omega_s \tag{41}$$

$$\vdots \tag{42}$$

The matched filter term in equation (36) has a spectral width that is narrower than that of the sampled spectrum by the over-sampling ratio. As ω_D is varied, the matched filter scans across the spectrum and wraps across the sampling window at $|\omega_D + \Omega| \geq \Omega_s$. The domains of interest are as follows:

- $|\Omega + \omega_D| < \Omega_s$, the unambiguous image domain
- $\Omega_s - 2\Omega \leq |\Omega + \omega_D| < \Omega_s + 2\Omega$, the wrapped image domain
- $\Omega_s \leq |\Omega + \omega_D| < 3\Omega_s$, the ambiguous image domain

In the ambiguous image domain two factors become important:

- For $\Omega_s \leq |\omega_D| < 2\Omega_s$ the apparent sign of the sampled representation of ω_D in the matched filter is reversed and its apparent value decreases as $2\Omega_s \text{sgn}(\omega_D) - \omega_D$ as ω_D increases. This is the direction ambiguity region of ω_D.
- For $2\Omega_s \leq |\omega_D| < 3\Omega_s$ the sign and direction of increase of the sampled and real ω_D correspond to each other.

The behaviour of the amplitude terms of (36) is illustrated in Figure 5.

In figure 5, the sampling window is wider than the matched filter window and, over the unambiguous image domain ($|\Omega + \omega_D \text{sgn}(\omega_D)| < \Omega_s$ the matched filter selects frequency offset portions of the sampled spectrum without any impact on the spectral width of the filter. In this domain, except for possible phase focus constraints, the resolution of the image is not affected by changes in ω_D, but the image amplitude decreases as ω_D approaches its positive and negative extremes due to the shape of the captured image spectrum. In addition the asymmetry of the image spectrum will increase the side-lobes of each focused point. The increased side-lobe content of the image will increase the integrated side-lobe ratio of the image and will decrease the image contrast. When $\omega_D \neq 0$, the shift in the centre frequency of the image spectrum will appear as a spatial shift in the focused image.

When $\Omega_s - 2\Omega \leq |\Omega + \omega_D \text{sgn}(\omega_D)| < \Omega_s + 2\Omega$, the sampling process wraps the matched filter, and thus the image spectrum as shown in the lower half of figure 5. The result is two superimposed images, an unambiguous image and an ambiguous image that are displaced from each other by their centre frequencies (and are spatially offset). The wrapping affect reduces the spectral width of each component with a resulting broadening of the impulse response for each point, reduction in the impulse response amplitude, and reduction in image contrast. When $\omega_D = \Omega_s$, the unambiguous and ambiguous images have equal magnitude and are superimposed but are oppositely offset from the centred, unambiguous image. As each of the image spectra for this case are half of the width of the original, unambiguous spectrum, the image impulse response functions are broadened by a factor of 2.

As ω_D continues to increase, the unambiguous spectrum shrinks, the unambiguous image impulse responses broaden and reduce in magnitude and the amplitude of the unambiguous image decreases.

When $\Omega_s \leq |2\Omega + \omega_D \text{sgn}(\omega_D)| < 3\Omega_s$, the ambiguous image spectrum replaces the unambiguous image spectrum at the top of figure 5 and no image defocus effects are caused by the sampled spectrum width (phase mismatch effects remain).

3.2 Terrain Spectral Phase terms

The phase terms for a stationary world focused by a moving target matched filter are qualitatively similar to the mismatched target case discussed in section 2.8.2. Again, the active image spectrum is governed by the intersections of the sampled spectrum and moving-target spectrum impulse functions, which are now $P_{\Omega_s}(\omega)$ and $P_{\Omega}(\omega + \omega_D)$ respectively.

To simplify the expressions for the sampled image spectra, set:

$$\Omega_1 = \Omega; \quad \forall\{|\omega_D| + \Omega \leq \Omega_s\} \tag{43}$$

$$\Omega_1 = \frac{\Omega_s + \Omega - \omega_d \text{sgn}(\omega_D)}{2}; \quad \forall\{\Omega_s < |\omega_D| + \Omega \leq \Omega_s + 2\Omega\} \tag{44}$$

$$\Omega_2 = \Omega - \Omega_1 \tag{45}$$

The spectral translation caused by increasing $|\omega_D|$ partitions the matched filter impulse function into two functions, $P_{\Omega_1}()$ and $P_{\Omega_2}()$. Noting that $P_0() = 0$, all cases are appropriately covered. The wrapping of the matched filter spectrum illustrated in figure 5 decomposes the impulse function, $P_{\Omega}(\omega + \omega_D)$ into the sum $P_{\Omega_1}(\omega + \omega_{D1}) + P_{\Omega_2}(\omega + \omega_{D2})$ where each of the partitions, P_{Ω_1} and P_{Ω_2} has its own phase function that is frequency offset from zero by the frequency corresponding to the midpoint of the active frequency interval.

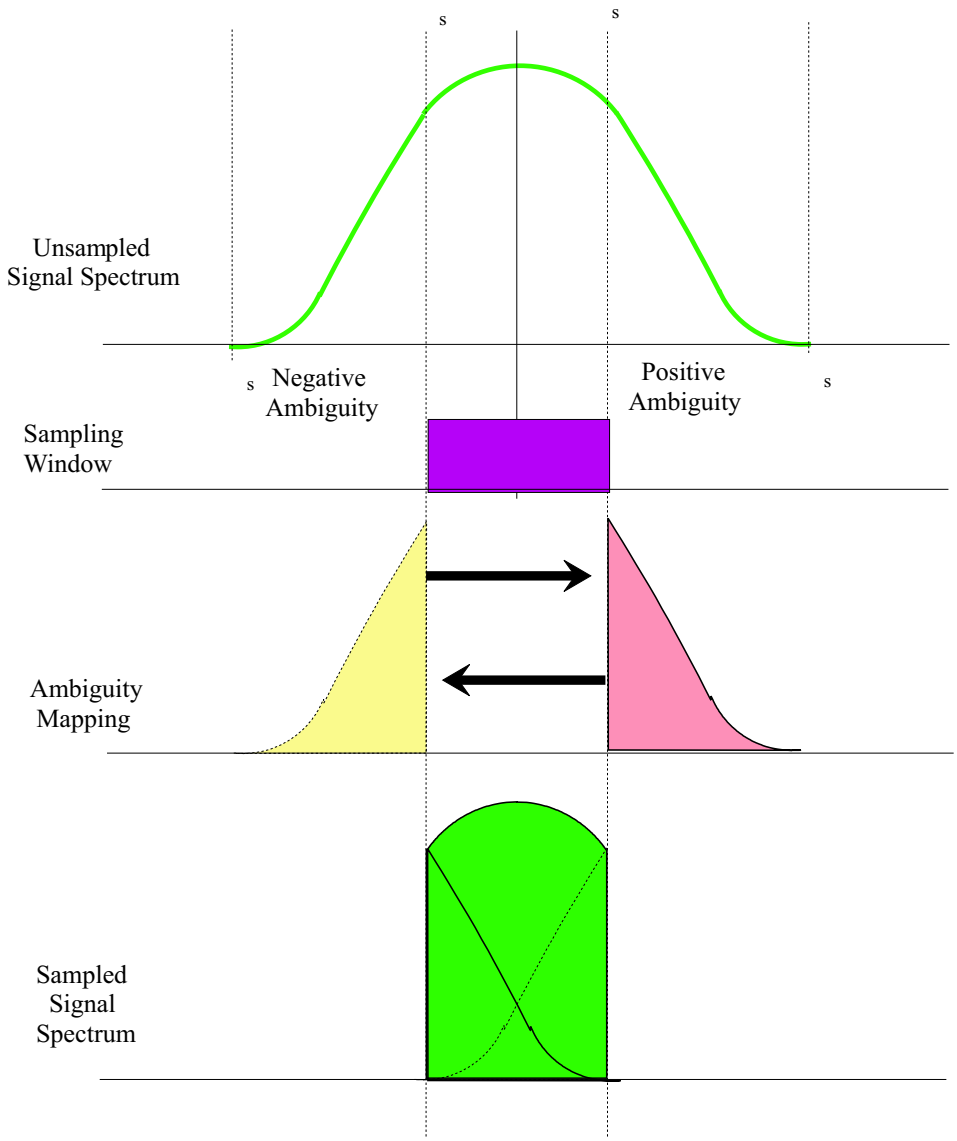

Figure 5: *Schematic representation of a sampled, stationary world signal spectrum formed into shifted image spectra by a sampled, moving-target matched filter. The over-sampling ratio shown is approximately 1.45*

For all $|\Omega + \omega_D| \leq \Omega_s$ the centre of the image spectrum is $\omega_D = \omega_{D1}$. Otherwise, the splitting of the matched filter caused by the sampling creates an image that is the sum of two separated spectral intervals, each with its own centre frequency.

$$\omega_{D1} = (\Omega_s - \Omega)\text{sgn}(\omega_D), \quad \forall\{\Omega_s < \Omega + |\omega_D| < \Omega_s + 2\Omega\} \tag{46}$$

$$\omega_{D2} = (\Omega_s - \Omega)\text{sgn}(\omega_D) \tag{47}$$

When ω_D is large enough to generate the fully ambiguous matched-filter case, $|\Omega + \omega_D| > \Omega_s + 2\Omega$, ω_D is replaced by $\omega'_D = -2\Omega_s + \omega_D$ in the sampled signal domain and equations (45) and (47) apply with magnitudes represented by ω'_D but signs determined by ω_D.

Returning to equation (36) and absorbing the constants into A(ω), we can write the image spectrum as:

$$\begin{aligned} I(f) = A(\omega)P_{\Omega_s}(\omega)\Bigg(& P_{\Omega_1}(\omega + \omega_{D1})P_\Omega(\omega)\exp j\left(\frac{\omega^2}{4k_0^2} - \frac{(\omega + \omega_{D1})^2}{4k_0\alpha}\right) \\ & + P_{\Omega_2}(\omega + \omega_{D2})P_\Omega(\omega)\exp j\left(\frac{\omega^2}{4k_0^2} - \frac{(\omega + \omega_{D2})^2}{4k_0\alpha}\right)\Bigg) \end{aligned} \tag{48}$$

In (48), the composite structure of the sampled signal spectrum given by (38) is contained within $A(\omega)$ and only the unambiguous spectrum is shown in the phase terms. The complete expression for the image spectrum can be expressed as the sum

$$I(\omega) = I_0(\omega_0) + \sum_{n=1}^{N}\left(I_{n+}(\omega_{n+}) + I_{n-}(\omega_{n-})\right) \tag{49}$$

where the notation and frequency intervals are defined in (42). A typical SAR image will contain the sum of ambiguous and unambiguous images where the ambiguous images are displaced in the image plane by an azimuth distance that corresponds to the frequency offset of the ambiguity.

Expanding the phase terms of (48), we get results that are similar to equations (23) and (24) in section 2.8.2

$$\phi_1(\omega) = \frac{1}{4k_0}\left[\omega^2 - (\omega^2 + 2\omega\omega_{D1} + \omega_{D1}^2)\left(1 - 2\frac{V_x}{V_a} + \frac{V_x^2}{V_a^2} + \frac{V_y^2}{V_a^2}\right)\right] \tag{50}$$

and

$$\phi_2(\omega) = \frac{1}{4k_0}\left[\omega^2 - (\omega^2 + 2\omega\omega_{D2} + \omega_{D2}^2)\left(1 - 2\frac{V_x}{V_a} + \frac{V_x^2}{V_a^2} + \frac{V_y^2}{V_a^2}\right)\right] \tag{51}$$

As with the case of a moving target imaged by a stationary-world matched filter, we have two cases of interest, $V_x = 0$ and $V_y = 0$.

3.2.1 The radial velocity case

Starting with V_x = 0

$$\phi_1(\omega) = -\frac{1}{4k_0}\left[\omega^2\frac{V_y^2}{V_a^2} + 2\omega\omega_{D1}\left(1+\frac{V_y^2}{V_a^2}\right) + \omega_{D1}^2\left(1+\frac{V_y^2}{V_a^2}\right)\right] \qquad (52)$$

The equation for $\phi_2(\omega)$ is identical to (52) with ω_{D1} replaced by ω_{D2}. As in section 2.8.2.1, the first term in (52) is a focus error term and defines the focus constraint arising from the mismatch between the moving-target-matched-filter and the stationary terrain spectrum. As the focus constraint is symmetric with respect to the source of the filter mismatch, (26) applies and phase mismatch effects only affect the image focus when V_y/V_a is large and are most important at long range. For the unambiguous spectrum, the terrain impulse response width and thus the image contrast is dominated by the bandwidth $2\Omega_1$. The image amplitude is determined by the spectral energy selected by $\mathrm{P}_{\Omega 1}(\omega + \omega_{D1})$. The same arguments apply for $\phi_2(\omega)$.

The second term of (52) defines the time-frequency product of the form $t_0\omega = \omega_{D1}/2k_0(1 + V_y^2/V_a^2)$ and in image formation, under the time shifting theorem of the Fourier transform results in a time (image azimuth) shift of the resulting image. For a stationary world imaged with a moving target matched filter, the unambiguous image has two cases:

For $\Omega + |\omega_D| \leq \Omega_s$, $\omega_{D1} = \omega_D$ and

$$t_0\omega = \frac{\omega_D}{2k_0}\left(1+\frac{V_y^2}{V_a^2}\right) \qquad (53)$$

as was seen in (26). For $\Omega_s < \Omega + |\omega_D| < \Omega_s + 2\Omega$, expanding ω_{D1} we have

$$t_1 = \frac{\omega_{D1}}{2k_0}\left(1+\frac{V_y^2}{V_a^2}\right) = \frac{(\Omega_s - \Omega)\mathrm{sgn}(\omega_D) + \omega_D}{4k_0}\left(1+\frac{V_y^2}{V_a^2}\right) \qquad (54)$$

From (54), when ω_D becomes large enough, $\Omega_1 < \Omega$ and $\omega_{D1} < \omega_D$. t_1 reaches its maximum value just as $\Omega_1 = 0$ ($|\omega_D| = \Omega_s + 2\Omega$). At this point $P_{\Omega_1}(\omega + \omega_D) = 0$ and the unambiguous image terms vanish.

Returning to (52) modified for ϕ_2, ω_{D1} is replaced by ω_{D2}. For the condition $|\Omega + \omega_D| \leq \Omega_s$, $\omega_{D1} = \omega_D$, $P_{\Omega_2} = 0$ and there is no wrapped signal. When $\Omega_s < \Omega + |\omega_D| < \Omega_s + 2\Omega$, $P_{\Omega_2} > 0$ and we have a wrapped, ambiguous signal whose frequency offset is

$$\omega_{D2} = \frac{(\Omega - 3\Omega_s)\mathrm{sgn}(\omega_D) + \omega_D}{2} \qquad (55)$$

and the corresponding image time (space) offset is

$$t_2 = \frac{\omega_{D2}}{2k_0}\left(1+\frac{V_y^2}{V_a^2}\right) = \frac{(\Omega_s-\Omega)\text{sgn}(\omega_D)+\omega_D}{4k_0}\left(1+\frac{V_y^2}{V_a^2}\right) \tag{56}$$

Examining (45), (47) and (55), the effective value of ω_D in the fully unambiguous and fully ambiguous sampled image spectra is $\omega_D' = \omega_D - 2N\Omega_s\text{sgn}(\omega_D)$ where N is the order of the ambiguity. In the transition (wrapping) intervals, both equations (54) and (56) define the image displacement in terms of the geometrical centre of the spectral interval. A better estimate takes into account the effective motion of the scene centroid defined by the spectral weighting (amplitude distribution) and the wrapped filter function. This will be of greatest significance for the spectra of the scene sampling ambiguities referenced in (49).

The third term of (52) is the residual phase for the scene and has the form:

$$\phi_{1,2} = \frac{\omega_{D1,2}^2}{4k_0}\left[1+\frac{V_y^2}{V_a^2}\right] \tag{57}$$

As the image wraps with increasing $|\omega_D|$, there is a phase jump between the ambiguous and unambiguous images of

$$\phi_1 - \phi_2 = \frac{\Omega_s^2}{4k_0}\left[1+\frac{V_y^2}{V_a^2}\right]\left(-2+\frac{\Omega}{\Omega_s}+\left(\frac{\omega_D}{\Omega_s}\left\{2-\frac{\Omega}{\Omega_s}\right\}\right)\right) \tag{58}$$

The phase difference has several interesting properties:

- It depends on the sampling frequency
- It is a function of the over-sampling ratio
- It changes with the order of the matched-filter ambiguity (integer part of ω_D/Ω_s)

The phase function, ϕ_1, has similar dependence on the sampling frequency on the over-sampling ratio and on the ambiguity order.

Returning to (38), (42) and figure 5 we see that the ambiguous components of the sampled signal interact with the matched filter most strongly on the P_{Ω_2} side of the image spectrum when $\omega_D \approx n\Omega_s \quad (n = \pm 1, \pm 2, \text{etc})$. Noting that $\int_{\Omega/2} A_{+,-}(\omega - \Omega_s) \ll \int_{\Omega/2} A_0(\omega - \Omega_s)$, the ambiguous components of the sampled scene spectrum will generally yield weak responses superimposed on the unambiguous scene. Where the imaged scene contains strong, ambiguous targets, these will appear as ambiguities, especially in cases where the unambiguous scene returns are weak. The moving target matched filter phase will preferentially focus the ambiguous scene content over appropriate ranges of ω_D.

3.2.2 The tangential velocity case

When we apply the condition $V_y = 0$ to equations (50) and (51) we have a case very similar to that discussed in section 2.8.2.2, ω_D = 0 and only focus terms survive. In this case the focus phase constraint discussion of section 2.8.2.2 applies to the scene as opposed to the target and increasing mismatch between the moving-target matched filter and the stationary world scene results in scene defocus and contrast loss.

4 Summary of SAR Azimuth Ambiguities for targets and terrain

The discussions in this note look at the case where the SAR data is range-compressed and there are no range ambiguities that have sufficient power to be considered. The analysis assumes an airborne radar system. This summary reviews the results from sections 2 and 3.

In sections 2.8, 3.1 and 3.2 two problems are considered:

- SAR processing of a moving target with a stationary-world matched filter
- SAR processing of a stationary world with a moving target matched filter.

A third problem SAR, processing of moving targets in a stationary world with a filter that is mismatched to both, was not discussed but can be inferred from the other two discussions.

Starting from the case of a radially moving target imaged by a stationary world matched filter (SWMF), the target signature has the shape defined by the radar antenna pattern convolved with the azimuth scattering pattern of the target (We will assume an ideal, point target.), has a spectrum centred at the target Doppler frequency, ω_D, and is sampled at frequency Ω_s. The matched filter has bandwidth Ω and is centred at 0. From the discussions in section 2.8 we see the following properties that are related to the sampling of the target signature:

1. The target is unambiguously captured by the matched filter over the Doppler frequency ranges $|\omega_D| < \Omega_s - \Omega$, as can be seen in figure 3. In the focused image, the target is displaced in azimuth by time t_0, (28), which is seen in the image as a displacement of $N_T = t_0/\Delta t$ for image sampling interval Δt. Noting that $\omega_D \propto V_y/V_a$, as ω_D increases to the point where the focus constraint, $\omega_f < \Omega$, (26), the target focus degrades and its amplitude decreases (this is

most significant for airborne SARs because of their relatively slow platform velocities). Depending on the magnitude of the over-sampling ratio, the antenna pattern weighting may significantly decrease the target amplitude near the upper and lower edges of the unambiguous target velocity range. In addition, there are two "dead bands", $-\Omega_s < \omega + \omega_D < -\Omega$ and $\Omega < \omega + \omega_D < \Omega_s$, that are not processed by the matched filter and signal energy in these bands is not included in the target image.

2. The target is split into ambiguous and unambiguous target images over the Doppler frequency ranges Ω_s - Ω < $|\omega_D|$ < Ω_s + Ω (figure 3) by the wrapping of the target spectrum caused by the sampling process. In the focused image, the unambiguous target is displaced by time t_1 (eqn 26) which is seen as a displacement of $N_T = t_1 / \Delta t$ and the ambiguous target is displaced in the opposite direction by time t'$_0$ (eqn 27) or $N_T = t_0' / \Delta t$ cells. As $|\omega_D|$ increases from Ω_s - Ω, the ambiguous target is very much weaker than the unambiguous target but increases in strength until the two have equal magnitude and opposite displacement at $|\omega_D|$ = Ω_s. At $|\omega_D| = \Omega_s$ the magnitude of each two target images is less than $1/\sqrt{2}$ of the magnitude of a stationary target of the same cross section due to defocusing effects and due to the un-processed target signal that results from the over-sampling ratio. As $|\omega_D|$ increases further towards its upper limit for this domain, the unambiguous target strength decreases and the strength of the ambiguous target increases in response to the widths of their respective impulse functions. As $|\omega_D|$ increases, the target focus constraint becomes increasingly significant (especially for airborne SAR platforms) and the target strength declines due to defocus effects. In the "split target" domain the target displacement in the focused image is less than that expected from the magnitude of the Doppler shift of the unsampled signal.

3. When $|\omega_D|$ >Ω_s + Ω, a single, fully ambiguous target remains whose sampled Doppler shift is $\omega_D'' = -2\Omega_s \text{sgn}(\omega_D) + \omega_D$ and the target behaviour reverts to the unambiguous case but with significant defocus (for airborne platforms).

4. The case of a tangentially moving target, as discussed in section 2.8.2.2, invokes only a defocus constraint as shown in equations (33) and (34) and has not displacement. As the tangential-motion defocus constraint is significantly more sensitive to the target velocity than is the radial-motion defocus constraint, the effects can be significant for space-based sensors.

The case of a stationary world imaged by a moving target matched filter (MTMF) is very similar to that of a moving target imaged by a stationary world matched filter (SWMF) except that in this case the sampled signal spectrum is fixed in the sample space and the matched filter impulse function moves with ω_D. Figure 5 provides a schematic visualisation of the spectra involved in the process. The same

qualitative effects, focus degradation (section 3.1, section 3.2), ambiguous image domains (section 3.1, eqn (45) and (47)), scene displacement (eqn (53), (54), (56)) are present for the background scene for the MTMF case as were seen for the moving target in the SWMF case (section 3.1, equations (53)-(56)). In the MTMF case, the impact of sampling on the capture of scene sampling ambiguities is expressed explicitly (eqn (38), (42), (49)). This effect also occurs in the SWMF case but is not shown explicitly in that discussion. The residual phase that arises from signal – processing filter phase mismatch is also expressed explicitly for the MTMF case (eqn (57) and (58)) and is shown to depend on the sampling frequency, the over-sampling ratio, and on the ambiguity order. The SWMF case also has a residual phase associated by the target – processing filter velocity mismatch.

Filling in data from the CV580 research system we have:

System parameters assumed:

- InSAR antenna sub-array beamwidth 5.2^0 (measured)
- Main antenna beamwidth 3.1^0 (measured)
- -6 dB 2-way beam-width 3.5^0
- Slant Range (R_0) 8000 m
- Altitude 6100 m
- Incidence angle (ψ) 40.3^0
- Ground speed (V_a) $=$ 128 m/s
- PRF/V 2.567 /m
- Wavelength (λ) 0.0567 m

Results from the SAR imaging/ambiguity calculations:

- PRF (double sampling rate) 657.2 Hz $\rightarrow \Omega_s$ = 2064.5 rad/s
- Maximum Doppler frequency (-6 dB)157.9 Hz $\rightarrow \Omega$ = 992.1 rad/s
- Over-sampling ratio 2.08
- FM constant (k_0) 226.9 s^{-2}
- Focus constraint V_y $=$2.44 m/s
- Focus constraint radial velocity 1.86 m/s

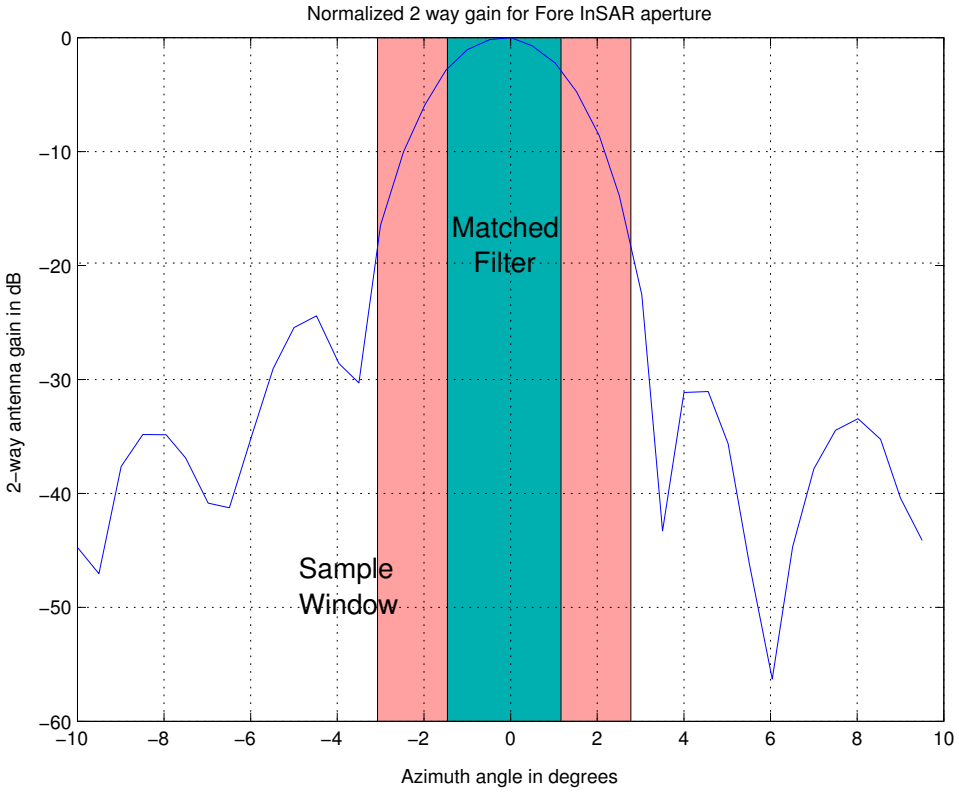

Figure 6: *CV 580 2-way antenna pattern for the Fore InSAR aperture showing the stationary-world matched-filter and the signal sampling intervals. This corresponds to the* ω_D *= 0 case shown schematically in figure 5*

- Ambiguity onset Doppler 170.7 Hz
- Ambiguity onset radial velocity 9.7 m/s
- Full ambiguity Doppler 486.5 Hz
- Radial velocity at full ambiguity 27.6 m/s

5 The SAR-MTI problem

For this section we will deal with the two-aperture SAR problem that corresponds to the CV 580 SAR and RADARSAT-2. Two-aperture MTI measures the short-term changes within a radar data set over the time interval required for the Aft aperture of the radar to be displaced into the position formerly occupied by the Fore aperture. For the CV 580 example case discussed in the last section, the aperture phase-centres are separated by 0.27 m and the corresponding time is 2.1 ms at a platform speed of 128 m/s. For SAR-GMTI, each aperture defines a separate radar and each generates a separate SAR image (if this processing mode is used). As the radar hardware is not ideal, there will be systematic differences in amplitude and phase between the two radar channels. When the details of the antenna apertures and radome (airborne case) are considered, there will be different, systematic variations over the two scenes that need to be compensated before GMTI analysis can proceed, [3, 4]. For the airborne case, the interaction between the antenna and the radome can result in structured phase difference behaviour as seen in Figure 7 as modelled by Gong for along-track SAR interferograms (SAR ATI).

5.1 GMTI pre-processing steps

Since the data needed to measure target motion is supplied by two “different” radars that simultaneously acquire spatially-offset data, two separate processing steps are required:

- The data from the two channels must be balanced in amplitude and phase to remove systematic components imposed by the radar equipment.
- The data from the two channels must be registered in time (one channel shifted and resampled) to place the Fore and Aft channels in the same spatial location for each radar pulse.

The order in which channel balancing and registration are accomplished, and the way in which the data are registered and resampled, can have an important impact on the resulting moving target measurements. There are two options:

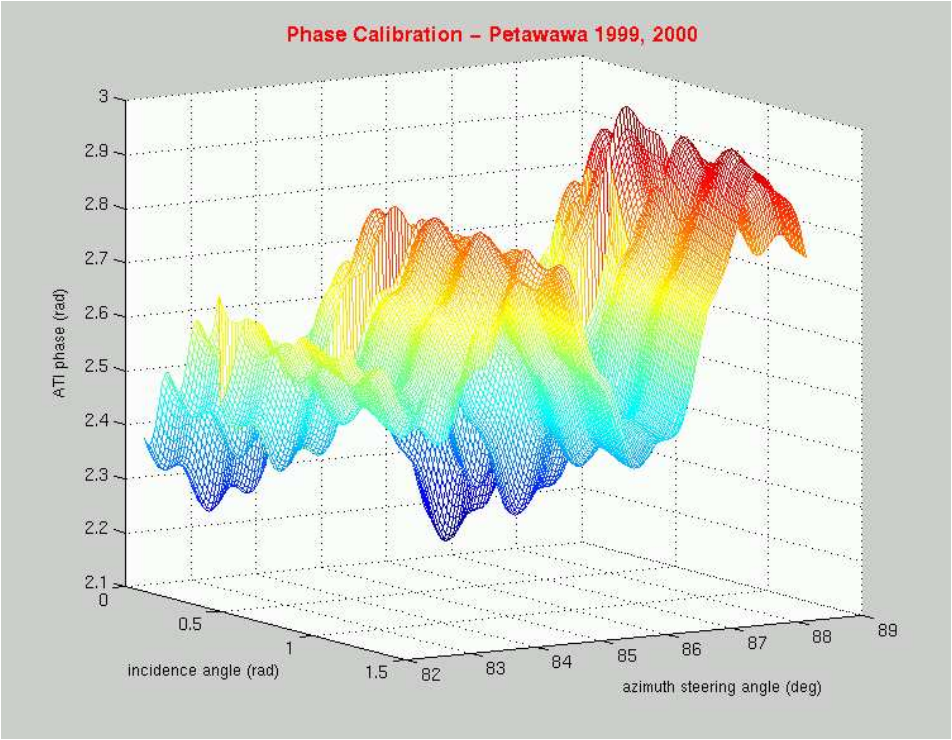

Figure 7: *Phase structure imposed on SAR ATI data by the antenna-radome interaction for the CV 580 SAR system*

- Perform the channel balancing on the simultaneously received data from the fore and aft apertures. Then perform the channel registration by matching the aft channel to the fore channel.

- Perform the channel registration and then balance the registered channels.

The first option has the advantage that any temporal variation in the radar or the scene is removed from consideration. The disadvantage is that the two beam margins may not exactly overlap. As this approach provides the maximum isolation between the radar system and the scene properties, it is preferred.

The second option has the advantage that the beam registration is as good as it will get. It has the disadvantage that temporal variations in the scene or in the radar are convolved into the balancing process.

In the first option, any residual phase shifts that result from radar ambiguities are preserved in the phase of the interferometric scene as reported by [5, 4, 6]. These must then be removed by modelling the imaging process to return the phase of the stationary world to zero when moving target matched filters wrap to ambiguous frequency offsets.

The registration of the Fore and Aft interferometer channels can be accomplished in the time domain by shifting and resampling one data channel or can be accomplished in the frequency domain by applying a phase multiplication to one channel (time shifting property of the Fourier transform).

5.2 GMTI Ambiguities

Once the preprocessing steps have been completed, the SAR data can be processed to form image data sets and the processed, registered SAR scenes can be analysed to detect and measure moving targets by correlation (ATI) or by subtraction (displaced phase centre antenna (DPCA)). When the SAR spectrum for each channel is processed to form a single image, the radial velocity of moving targets within the scene pair is measured as the change in the target range in the time interval between the radar apertures (DPCA time). This is measured in fractional wavelengths as a phase angle. The periodic nature of angle measurements imposes an ATI ambiguity on the velocity measurement process. Unless very restrictive conditions are imposed (phase centre separation is equal to the effective sub-aperture length and the over-sampling ration is unity) the ATI ambiguities occur at different target velocities than the sampling ambiguities.

If the phase centre separation distance in the platform motion direction is d and the airborne platform velocity is V_a the DPCA time is $\tau = d/V_a$ and the radial velocity,

V_R, of the target is ambiguous whenever

$$2V_R\tau = \delta R_{Targ} = \frac{d2V_R}{V_a} = \frac{n\lambda}{2} \tag{59}$$

There are two classes of ATI ambiguity:

- When n is odd, the direction of motion of the target is ambiguous and a target moving towards the radar at one speed has the same phase as a target moving away from the radar at a different speed.
- When n is even, the target phase does not change between the two apertures (there is no apparent target motion). These are the "blind" speeds of the radar.

As the synthetic aperture time of the radar, $T = R\Theta_0/V_a$, is much larger than the DPCA time, τ, these ambiguities can be resolved if the radar bandwidth is sufficiently large. If the spectra from the Fore and Aft apertures are each filtered in the azimuth direction to form Fore and Aft sub-beams (looks) and if the displacement of the target over the aperture time is greater than a significant fraction (say 1/2) of the sub-beam resolution, then processing the two sub-beams to SAR images, registering these, and subtracting them results in residual targets elongated or separated in the direction of motion.

5.3 ATI ambiguity Example

For the CV 580 radar parameters from section 4 with Fore and Aft aperture phase centre separation of 0.27 m, we see that the first directional ambiguity occurs at a target radial velocity of 6.7 m/s and the first blind-speed occurs at a target radial velocity of 13.4 m/s. These numbers compare with the onset of the sampling ambiguity region at a target radial velocity of 9.7m/s from section 4.

Taking the radar range resolution to be 5.7 m and filtering the antenna aperture beams into two contiguous sub-beams with 1.75^0 separation, the time between the sub-beam centres at 8000 m range is 1.9 seconds which translates into 2.23 resolution cells range-offset at the first directional ambiguity. This is more than adequate to resolve the ambiguity.

5.4 The impact of sampling ambiguities on ATI measurements.

From (58) we note that a velocity mismatch between the processing filter and the SAR scene results in a phase offset between the unambiguous and ambiguous images when the velocity is sufficiently large to excite that condition.

The analysis up to that point did not cover the two-aperture case and the registration operation required for MTI measurements. It was noted in section 5.1, that successive ambiguities caused by moving-target matched filters applied to the stationary world do result in steps in the stationary world ATI mean phase and that these steps are functions of the sampling rate of the radar.

6 Interferometric phase staircase effect for stationary terrain

Trials confirm the evidence of SAR processing ambiguities that stem from the sampled nature of both the SAR signal and the matched filter used for compression. Oddly, interferometric pairs show a phase jump at the junction between ambiguities. This “stepping” effect is illustrated in figure 8. By proceeding with an analysis

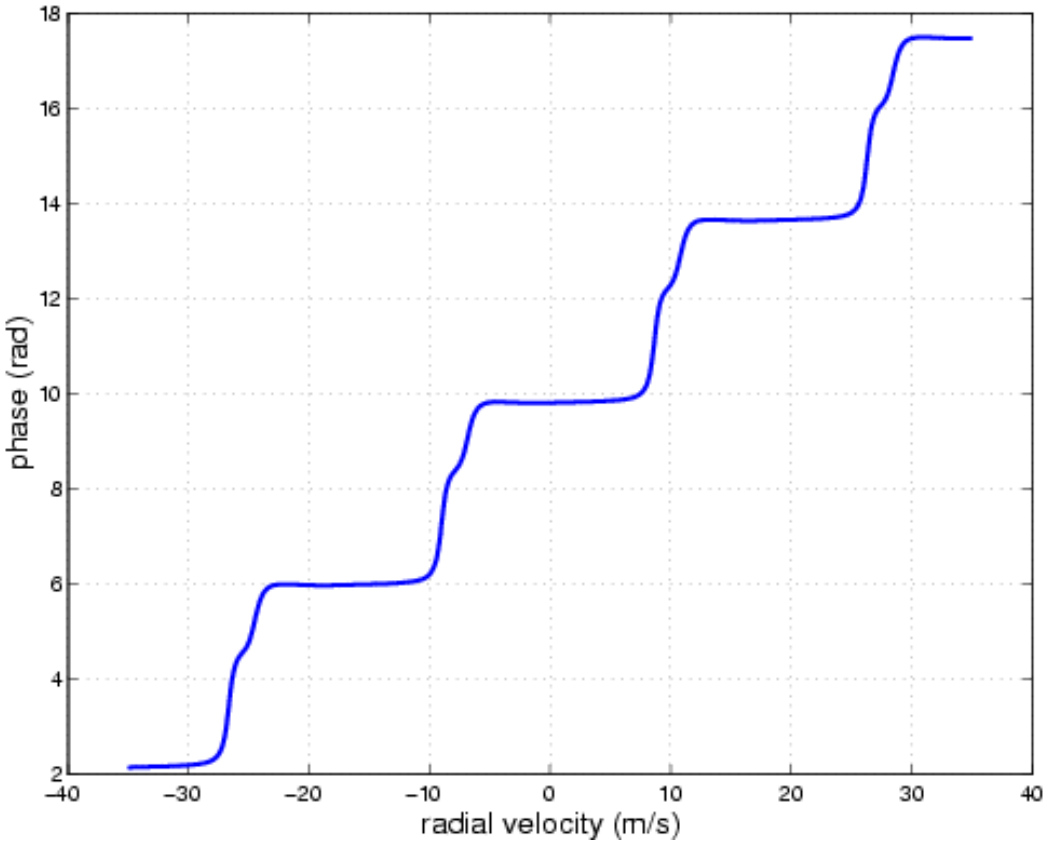

Figure 8: *Staircase effect for interferometric phase of stationary terrain.*

of the phases of the compressed signals, it becomes clear that the phase jumps are

due to the time resampling of one of the channels. The reason for actually doing the time resampling stems from the fact that the physical GMTI system consists of two antenna apertures aligned along-track that are designed to sample the returned signal at the same instant in time. In effect, the fore antenna measures what the aft antenna does at a later time. The difference in time is determined by how long it takes the aircraft to move the aft antenna into the previous position of the fore antenna. This time depends on the physical separation between the antenna phase centres and the speed of the aircraft. From a SAR processing point of view, this geometry is easy to accommodate; one simply processes the aft channel to return the response of the measurement at a delayed time.

7 Interpolation by delaying the reference function

As shown previously [7, 8], the phase of the reference function used for SAR compression is given by

$$r(t) = \exp\left[j\beta(\sqrt{(vt)^2 + (r_0 + \dot{r}t)^2} - r_0)\right], \tag{60}$$

where v is the aircraft velocity, r_0 is the target broadside range, $\beta = 4\pi/\lambda$, λ is the radar wavelength, and $\dot{r}$ is the target radial velocity. This equation can be understood by thinking of the target positioned at $r_0 + \dot{r}t$ in the slant range dimension, and the aircraft positioned at vt in the perpendicular along-track direction then just applying Pythagoras' theorem. In this model the aircraft sits at along track position, 0, when $t = 0$. Now, in order to know the response of SAR processing at a position displaced from $t = 0$, one only needs to introduce a time delay into the reference function. Spatially this delay is equivalent to the phase centre separation, d, but this corresponds to a time delay of d/v where v is the aircraft speed. Since we also want to place the target into the same time reference, the overall, new, reference function is

$$r(t) = \exp\left[j\beta(\sqrt{(v(t + d/v))^2 + (r_0 + \dot{r}(t + d/v))^2} - r_0)\right]. \tag{61}$$

Expansion of the square root function using $\sqrt{1+x} \approx 1 + 1/2x + \mathrm{O}(x^{-2})$ for $x << 0$ yields

$$r(t) \approx \exp\left[j\beta\left(\frac{v^2t^2}{2r_0} + t(\frac{vd}{r_0} + \dot{r} + \frac{\dot{r}^2 d}{vr_0}) + \frac{\dot{r}d}{v} + \frac{\dot{r}^2d^2}{2r_0v^2}\right)\right], \tag{62}$$

where we have thrown away a couple of very small terms.

Recall that in reality, only a sampled version of the signal is recorded, and in the computer, a sampled version of the reference function is used for compression. Let the sampling frequency be denoted by f_p so that $t = \frac{n}{f_p}$. Also recall that the recorded signal also has, effectively, compact support (so does the reference function). Therefore ensure this condition by multiplying (62) by a rect function:

$$r(n) = \text{rect}_L(n) \exp\left[j\beta \left(\frac{v^2 n^2}{2 r_0 f_p^2} + \frac{n}{f_p}\left(\frac{vd}{r_0} + \dot{r} + \frac{\dot{r}^2 d}{v r_0}\right) + \frac{\dot{r} d}{v} + \frac{\dot{r}^2 d^2}{2 r_0 v^2} \right) \right], \quad (63)$$

where,

$$\text{rect}_L(n) = \begin{cases} 1/L \ \text{ if } |n| \leq L \\ 0 \ \text{ otherwise} \end{cases} \quad (64)$$

Equation (63) is modelled on the actual recorded signal

$$s(n) = \text{rect}_L(n) \exp\left[-j\beta \left(r_0 + \frac{v^2 n^2}{2 r_0 f_p^2} + \frac{n}{f_p}\left(\frac{vd}{r_0} + \dot{y} + \frac{\dot{y}^2 d}{v r_0}\right) + \frac{\dot{y} d}{v} + \frac{\dot{y}^2 d^2}{2 r_0 v^2} \right) \right], \quad (65)$$

where $\dot{y}$ is the actual target radial velocity.

8 Azimuth compression

By viewing SAR compression as the application of a correlator [9], one can write the output of the compression as

$$c(m) = \sum_{-\infty}^{\infty} r(n) s(n+m), \quad (66)$$

however, because of the compact support, the infinite limits can really be replaced by some appropriate choice of $a \geq 0$ and $b \geq 0$ such that

$$c(m) = \sum_{-a}^{b} r(n) s(n+m). \quad (67)$$

Substitute this representation for the reference function, (63), and the signal, (65), into (67) to get

$$c(m) = \sum_{-a}^{b} \exp\left[j\beta\left(\frac{v^2n^2}{2r_0f_p^2} + \frac{n}{f_p}(\frac{vd}{r_0} + \dot{r} + \frac{\dot{r}^2d}{vr_0}) + \frac{\dot{r}d}{v} + \frac{\dot{r}^2d^2}{2r_0v^2}\right)\right] \tag{68}$$

$$\cdot \exp\left[-j\beta\left(r_0 + \frac{v^2(n+m)^2}{2r_0f_p^2} + \frac{(n+m)}{f_p}(\frac{vd}{r_0} + \dot{y} + \frac{\dot{y}^2d}{vr_0}) + \frac{\dot{y}d}{v} + \frac{\dot{y}^2d^2}{2r_0v^2}\right)\right] \tag{69}$$

$$= \exp\left[j\beta\left(-r_0 + \frac{\dot{r}d}{v} + \frac{\dot{r}^2d^2}{2r_0v^2} - \frac{v^2m^2}{2r_0f_p^2} - \frac{m}{f_p}(\frac{vd}{r_0} + \dot{y} + \frac{\dot{y}^2d^2}{vr_0}) - \frac{\dot{y}d}{v} - \frac{\dot{y}^2d^2}{2r_0v^2}\right)\right] \tag{70}$$

$$\cdot \sum_{-a}^{b} \exp\left[-j\beta n\left(\frac{v^2m}{r_0f_p^2} - \frac{1}{f_p}(\dot{r} - \dot{y} + \frac{\dot{r}^2d}{vr_0} - \frac{\dot{y}^2d}{vr_0})\right)\right]. \tag{71}$$

Careful examination of the sum shows that it is a finite geometric series [2] of $a + b + 1$ elements so one derives, for only the sum part that

$$\sum_{-a}^{b} \exp\left[-j\beta n\left(\frac{v^2m}{r_0f_p^2} - \frac{1}{f_p}(\dot{r} - \dot{y} + \frac{\dot{r}^2d}{vr_0} - \frac{\dot{y}^2d}{vr_0})\right)\right] \tag{72}$$

$$= \exp\left[j\beta\left(\frac{v^2m}{r_0f_p^2} - \frac{1}{f_p}(\dot{r} - \dot{y} + \frac{\dot{r}^2d}{vr_0} - \frac{\dot{y}^2d}{vr_0})\right)\left(\frac{a-b}{2}\right)\right] \tag{73}$$

$$\cdot \frac{\sin\left[\beta\left(\frac{v^2m}{r_0f_p^2} - \frac{1}{f_p}(\dot{r} - \dot{y} + \frac{\dot{r}^2d}{vr_0} - \frac{\dot{y}^2d}{vr_0})\right)(\frac{a+b+1}{2})\right]}{\sin\frac{\beta}{2}\left(\frac{v^2m}{r_0f_p^2} - \frac{1}{f_p}(\dot{r} - \dot{y} + \frac{\dot{r}^2d}{vr_0} - \frac{\dot{y}^2d}{vr_0})\right)}. \tag{74}$$

Overall, the output of the correlator will have a magnitude given by the ratio of sinusoids, and a phase given by

$$\Theta(m) = \left(\frac{a-b}{2}\right)\frac{\beta}{f_p}\left(\frac{v^2m}{r_0f_p} - \dot{r} + \dot{y} - \frac{\dot{r}^2d}{vr_0} + \frac{\dot{y}^2d}{vr_0}\right)$$
$$+ \beta\left(-r_0 + \frac{\dot{r}d}{v} + \frac{\dot{r}^2d^2}{2r_0v^2} - \frac{v^2m^2}{2r_0f_p^2} - \frac{m}{f_p}\left(\frac{vd}{r_0} + \dot{y} + \frac{\dot{y}^2d}{vr_0}\right) - \frac{\dot{y}d}{v} - \frac{\dot{y}^2d^2}{2r_0v^2}\right). \tag{75}$$

9 Target position and phase

Analysis of the correlator magnitude, given by

$$\frac{\sin\left[\beta\left(\frac{v^2m}{r_0f_p^2}-\frac{1}{f_p}(\dot{r}-\dot{y}+\frac{\dot{r}^2d}{vr_0}-\frac{\dot{y}^2d}{vr_0})\right)(\frac{a+b+1}{2})\right]}{\sin\frac{\beta}{2}\left(\frac{v^2m}{r_0f_p^2}-\frac{1}{f_p}(\dot{r}-\dot{y}+\frac{\dot{r}^2d}{vr_0}-\frac{\dot{y}^2d}{vr_0})\right)}, \tag{76}$$

by using L'Hôpital's rule reveals a maximum of $(a+b+1)/2$ when

$$\beta\left(\frac{v^2m}{r_0f_p^2}-\frac{1}{f_p}(\dot{r}-\dot{y}+\frac{\dot{r}^2d}{vr_0}-\frac{\dot{y}^2d}{vr_0})\right)\rightarrow 2k\pi \tag{77}$$

It is this periodicity that gives rise to SAR image ambiguities. The greatest maximum occurs when there is maximal overlap between the recorded SAR signal and the reference function. At this point, one finds that $a = b$ at half the length of the reference function and that $m = 0$. With these values, one realizes that if the condition

$$\dot{r}-\dot{y}+\frac{d}{vr_0}(\dot{r}^2-\dot{y}^2)=\frac{2k\pi f_p}{\beta} \tag{78}$$

is satisfied, then the maximum will be achieved. When the maximum is obtained, the predicted phase will be

$$\Theta(0)=-\beta r_0+2k\pi d\frac{f_p}{v}. \tag{79}$$

In words, a suitable choice for the reference function radial velocity can make it appear as though the SAR scene were processed with a stationary world matched filter. This appearance is only in the magnitude and position of the target. When $d \neq 0$, the symmetry is broken by the phase because it depends on k. Stated another way, $\exists\dot{r}$ such that $\forall k \in \mathcal{I}$, $m = 0$. Since $m = 0$, the target is always at the same position as it is in the stationary image, (which is $m = 0$), and has the same magnitude because of L'Hôpital's rule. The phase of the target, however, is not the same if $d \neq 0$. Recall that for different choices of $\dot{r}$, the position of the target in the compressed SAR image is seen to change. A natural question is why not choose a different $m \neq 0$ to satisfy condition (77)? The answer, of course, is that $m \leq L$ where $L < \infty$ because of the compact support of the recorded signal and reference function.

10 Phase jump on Convair 580 SAR-GMTI data

Data collected by the CV580 has either been collected with a f_p/v ratio of 5.14m^{-1} or 4.64m^{-1} [8]. It has also been determined that the phase centre separation is $d = 0.2704\text{m}$ [8]. These parameters lead to a phase jump of either $8.7327\text{rad} = -220^\circ$ or $7.8832\text{rad} = -268^\circ$ **only for** the channel which is time resampled. The channel which is not time resampled has $d = 0$, so the phase does not change with the ambiguity. An interferogram will, of course, show the phase jumps, and these precise values of -220° and -268°, have been noted with the CV580 SAR data, [6].

11 Effect on fast moving targets

Let us imagine that a moving target is situated in one of the ambiguities because of its radial velocity. Estimation of the radial velocity with the interferometric phase, even unwrapped, will **not** provide the correct radial velocity unless the phase jump is considered. Estimation of the radial velocity with non-coherent techniques such as time-frequency analysis or maximum likelihood will be free of the phase jump phenomenon, allowing the ambiguous region to be identified, which, in turn, will allow for correct accounting of the phase jump.

12 Summary

This technical memorandum provides a tutorial on the processing of synthetic aperture radar (SAR) ground moving target indication (GMTI) data with a filter that is not matched to the collected data. This occurs, for example, when objects in the terrain undergo motion that is not accounted for in the SAR filter. The effect of the mismatched filter manifests as defocussed targets if they have a significant tangential velocity, and, or displaced and ambiguous targets if they have an across-track velocity. Conversely, when the SAR filter has been modified to compress moving objects, the stationary contextual radar scene suffers from filter mismatch. Effects in this case include squinted imagery, and overlapping ambiguous images atop the stationary image.

This technical memorandum also addresses the issue of ambiguities arising from the sampling of the SAR signal. Two ambiguities are identified: one stemming from an ambiguous along-track interferometric phase measurement, the other from ambiguous targets in the SAR scene. We find that the processed radar data are

ambiguous in the across-track velocity used for processing, or in the across-track velocity that they actually possess. It is shown that the two types of ambiguity manifeset for different values of the across-track velocity.

References

1. Knight, T. and Sikaneta, I. C. (2000). Velocity offset processing. Internal web note, theory section.

2. Franceschetti, G. and Lanari, R. (1999). Synthetic Aperture RADAR PROCESSING, Washington: CRC Press.

3. Gong, S. (2001). Systematic Along-Track Interferometriy phase. Internal web note, theory section.

4. Gierull, C. H. (2003). Digital Channel Balancing of Along-Track Interferometric SAR Data. Defence Research and Development Canada. (Technical Memorandum TM 2003-024).

5. Sikaneta, I. C. (2001). Clutter phase rotation and baseline. Internal web note, theory section.

6. Gong, S. (2002). Experiment data analyzing report. Internal web note, theory section.

7. Sikaneta, I., Campbell, J., and Robson, M. (2001). The Airborne Along Track INSAR processor: Documentation, Guide, History. Defence Research and Development Canada. (Technical Memorandum TM 2001-053).

8. Livingstone, C.E., Sikaneta, I., Gierull, C.H., Chiu, S., Beaudoin, A., Campbell, J., Beaudoin, J., Gong, S., and Knight, T.A. (2002). An airborne synthetic aperture radar (SAR) experiment to support RADARSAT-2 ground moving target indication (GMTI). *Can. J. Rem. Sens.*, **28**(6), 1–20.

9. Ulaby, F. T., Moore, R. K., and Fung, A. K. (1986). Microwave Remote Sensing: active and Passive, Vol. 3. Reading, MA: Addison–Wesley.

DOCUMENT CONTROL DATA

(Security classification of title, body of abstract and indexing annotation must be entered when the overall document is classified)

1. ORIGINATOR (the name and address of the organization preparing the document. Organizations for whom the document was prepared, e.g. Establishment sponsoring a contractor's report, or tasking agency, are entered in section 8.)

Defence R&D Canada – Ottawa
3701 Carling Ave., Ottawa,
ON, K1A 0Z4

2. SECURITY CLASSIFICATION (overall security classification of the document, including special warning terms if applicable)

UNCLASSIFIED

3. TITLE (the complete document title as indicated on the title page. Its classification should be indicated by the appropriate abbreviation (S,C or U) in parentheses after the title.)

Focusing moving targets / terrain imaged with moving-target matched filters: A tutorial

4. AUTHORS (Last name, first name, middle initial)

Livingstone, Chuck and Sikaneta, Ishuwa

5. DATE OF PUBLICATION (month and year of publication of document)	6a. NO. OF PAGES (total containing information. Include Annexes, Appendices, etc.)	6b. NO. OF REFS (total cited in document)
September, 2004	45	9

7. DESCRIPTIVE NOTES (the category of the document, e.g. technical report, technical note or memorandum. If appropriate, enter the type of report, e.g. interim, progress, summary, annual or final. Give the inclusive dates when a specific reporting period is covered.)

Technical Memorandum

8. SPONSORING ACTIVITY (the name of the department project office or laboratory sponsoring the research and development. Include the address.)

DRDC Ottawa
2701 Carling Ave.
Ottawa, ON, K1A 0Z4

9a. PROJECT OR GRANT NO. (if appropriate, the applicable research and development project or grant number under which the document was written. Please specify whether project or grant)	9b. CONTRACT NO. (if appropriate, the applicable number under which the document was written)
15eg11	

10a. ORIGINATOR'S DOCUMENT NUMBER (the official document number by which the document is identified by the originating activity. This number must be unique to this document.)	10b. OTHER DOCUMENT NOS. (Any other numbers which may be assigned this document either by the originator or by the sponsor)
DRDC Ottawa TM 2004-160	

11. DOCUMENT AVAILABILITY (any limitations on further dissemination of the document, other than those imposed by security classification)

(X) Unlimited distribution
( ) Distribution limited to defence departments and defence contractors; further distribution only as approved
( ) Distribution limited to defence departments and Canadian defence contractors; further distribution only as approved
( ) Distribution limited to government departments and agencies; further distribution only as approved
( ) Distribution limited to defence departments; further distribution only as approved
( ) Other (please specify):

12. DOCUMENT ANNOUNCEMENT (any limitation to the bibliographic announcement of this document. This will normally correspond to the Document Availability (11). However, where further distribution (beyond the audience specified in 11) is possible, a wider announcement audience may be selected.)

13. ABSTRACT (a brief and factual summary of the document. It may also appear elsewhere in the body of the document itself. It is highly desirable that the abstract of classified documents be unclassified. Each paragraph of the abstract shall begin with an indication of the security classification of the information in the paragraph (unless the document itself is unclassified) represented as (S), (C), or (U). It is not necessary to include here abstracts in both official languages unless the text is bilingual).

This technical memorandum provides a tutorial on the processing of synthetic aperture radar (SAR) ground moving target indication (GMTI) data with a filter that is not matched to the collected data. This could occur, for example, when objects in the terrain undergo motion that is not accounted for in the SAR filter. Or, conversely, when the SAR filter has been modified to compress moving objects thereby introducing a mismatch with stationary objects.

Additionally, due to the sampling of the SAR signal, ambiguities become an issue. The matched filter to properly focus an image is not unique. It is possible that a filter constructed with a given across-track velocity parameter yields a SAR image that cannot be distinguished from the SAR image constructed with a filter identical in all respects except for a different but appropriately chosen across-track velocity paramter. This technical memorandum explores the ambiguity issue and discusses the impact on SAR-GMTI.

14. KEYWORDS, DESCRIPTORS or IDENTIFIERS (technically meaningful terms or short phrases that characterize a document and could be helpful in cataloguing the document. They should be selected so that no security classification is required. Identifiers such as equipment model designation, trade name, military project code name, geographic location may also be included. If possible keywords should be selected from a published thesaurus. e.g. Thesaurus of Engineering and Scientific Terms (TEST) and that thesaurus-identified. If it is not possible to select indexing terms which are Unclassified, the classification of each should be indicated as with the title.)

SAR, Ambiguity, Interferometry, Matched-Fitlering

Defence R&D Canada

Canada's leader in defence
and national security R&D

R & D pour la défense Canada

Chef de file au Canada en R & D
pour la défense et la sécurité nationale

www.drdc-rddc.gc.ca